We thank referee #1 for the comments and suggestions. A point-to-point response is presented below. The author responses are in blue while the referee comments are in black. All line references are to the submitted revised copy.

The approach for retrieving bimodal lognormal stratospheric aerosol size distributions for sulfate and smoke aerosols has been carefully documented, tested, and validated using synthetic and observational multi–wavelength aerosol extinction measurements. Revisions are made to i) improve methodology descriptions, ii) highlight the novelty of the approach, and (iii) demonstrate the robustness with respect to the operational method.

#1. "In this paper, the authors attempt to develop a new approach for retrieving bimodal lognormal stratospheric aerosol size distributions from measured and simulated extinction spectra. However, the methodology is difficult to follow, and the novelty of the approach is not clear. The basic idea of fitting extinction spectra to theoretical Mie cross sections is well-known, and ill-constrained given the complexity of aerosol size, composition, etc."

Fitting extinction spectra to theoretical Mie cross-sections has a long history of application to satellite multi-wavelength observations, such as those from the SAGE mission. Given the complexity of aerosol size and composition, this underlying approach, despite being well-known**,** remains ill-constrained. Knepp et al. (2024), based on SAGE III/ISS, report that (i) smoke cannot be accurately portrayed by the operational aerosol product and (ii) retrieval of a bimodal distribution is both expensive and error prone. No current operational satellite retrieval techniques retrieve the aerosol size distribution using a bimodal lognormal distribution to describe stratospheric aerosols. Furthermore, historical and contemporary stratospheric aerosol size distribution retrievals assume only sulfate aerosols. In this study, a new technique for retrieving bimodal lognormal aerosol size distributions from satellite multi-wavelength extinction data is developed to characterize stratospheric aerosol properties with growing influence of wildfires contributing to aerosol concentrations.

In addition, we revised the manuscript to highlight the need for smoke-aware retrieval. These include:

- Recent decadal observations of smoke in the stratosphere shift the assumption of the typical aerosol composition in the stratosphere (new lines: 34–37), with smoke radiative and chemical impacts in the stratosphere, and extinction profiles, distinct from sulfate aerosols (new lines: 37–41, 72–75).
- There is a clear gap in operational solutions from satellite which match the long standing stratospheric aerosol in situ data record of polydisperse distributions (new lines: 47–52, 81–86, 95–98, 100–102, 109–114).

- There is a need to better characterize the aerosol properties of recent frequent and intense wildfire events transporting smoke into the stratosphere (new lines 59–63, 69–72, 75–76, 99–100).

Revisions to clarify the retrieval methodology are done. These include:

- The formulated extinction ratios from Mie Theory are unique for bimodal distributions due to the impacts of the large particle concentrations in new lines: 226–229, and amended fig. 2 in new lines: 233–239.
- The Angstrom exponent solution space used to retrieve characteristics of the course mode is more explicitly defined in new lines: 243–245, 247–248.

Figure C1a is the same as figure 2 in the original manuscript, using extinction ratios at 384/756 nm and 1544/756 nm to present the baseline solution space. Figure C1a shows the solution space used here to define the characteristics of the fine mode as extinction ratios are a function of the varying fine mode widths and median diameters assuming coarse mode number fraction is equal to 0. The figure presents an alternative to the 449/756 nm and 1544/756 nm extinction ratios presented for sulfate aerosols in Wrana et al., 2021, 2023, 2025 and in Knepp et al., 2024. Presented here additionally is the extinction ratios and fine mode characteristics for smoke aerosols, with both species calculated using refractive indices from OPAC (Hess et al., 1998) which are now shown in Table 1 on new lines: 214–215. The selected wavelength pairs used here (384/756 nm, 756/1544 nm) offer the best sensitivity to fine and coarse mode aerosols (see: Knepp et al., 2024 Table 4 for other wavelength combinations). Sensitivity of the 384/756 nm extinction ratio is identified in figure 1 and sect. 3 of the original manuscript. The key assumption made in figure C1a and in the referenced works by Wrana et al. and Knepp et al., is that the coarse mode fraction is equal to 0 and all aerosol concentrations are contained within a single mode. The referenced works use this solution space to infer characteristics of a unimodal lognormal size distribution.

Figure C1b presents the solution space for one variation of many, of the extinction ratios for a bimodal distribution, with a coarse mode fraction equal to 10 % and a coarse mode width equal to 1.05, with the same varying curves of the fine mode width and median diameter. Larger aerosols with higher extinction efficiencies exert a significant influence on aerosol extinction and is a widely accepted fundamental physical observation, displayed in this figure as changes to the extinction ratios from fig. C1a. Figure C1b is added to the manuscript as fig. 2b (new line: 234) and caption (new line: 235–239), and description (new line: 227–229). As stated in the original manuscript (new lines 226–227), consideration of a secondary (coarse) mode alters the extinction ratios and solution space used to define the characteristic fine mode here, and used to retrieve unimodal distributions in the works of Knepp et al., 2024 and Wrana et al., 2021, 2023, 2025. To this point, the overall methodological approach here determines the size distribution from the

extinction spectra, with high sensitivity to aerosol diameters within a strict bounded uncertainty range, and accounts for fundamental variances due to the sampled polydisperse aerosol population. This equates to more than a statistical optimization of the solution space while assuming only one mode in the aerosol population.

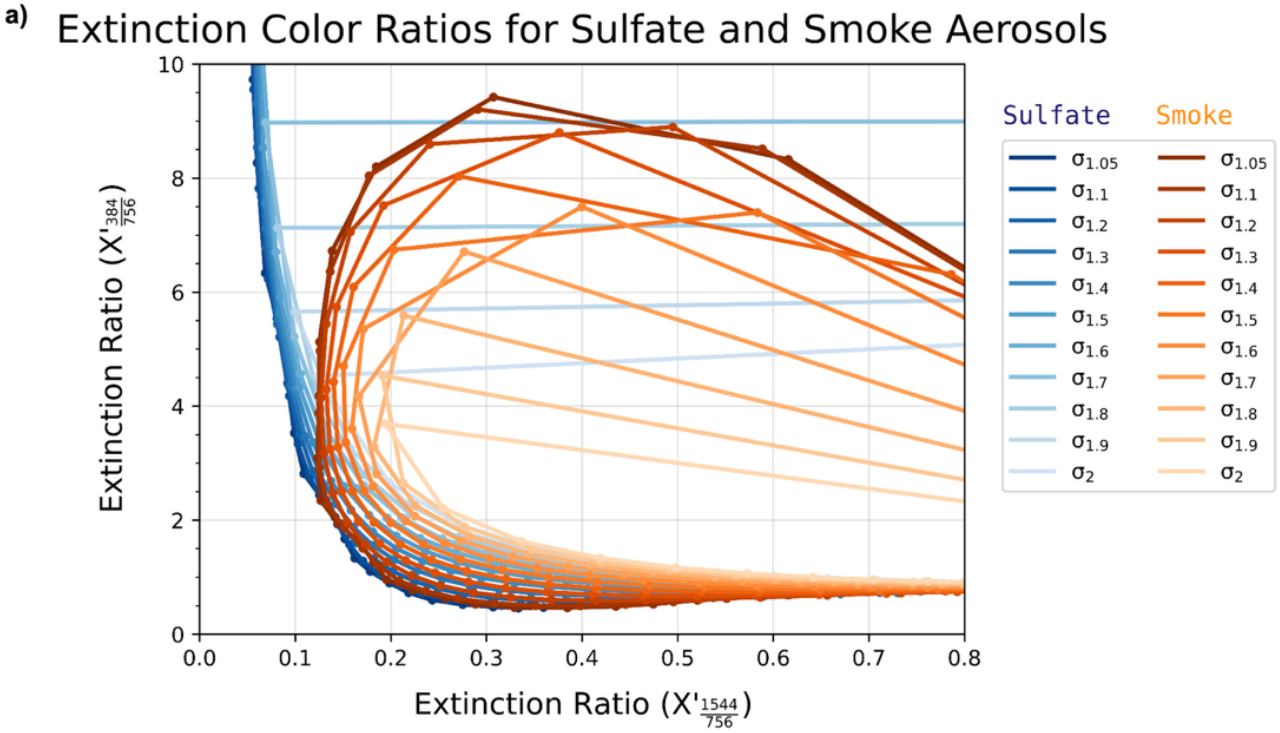

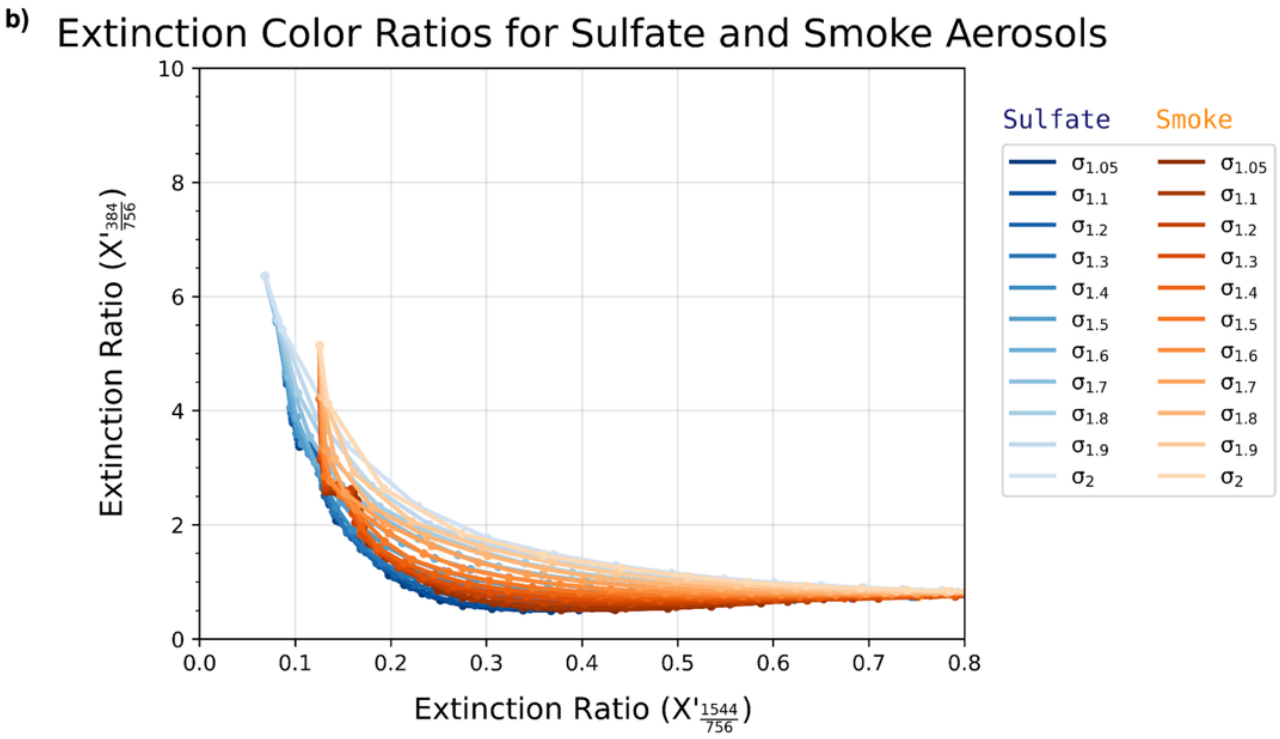

Figure C1: Extinction color ratios for sulfate and smoke aerosols using the 384/756 nm and 1544/756 nm wavelength pairs as a function of aerosol diameter. a) Assumes a coarse mode fraction (γ_{Coarse}) equal to 0, and b) Assumes γ_{Coarse} equal to 10 % and $\sigma_{g,\ Coarse}$ equal to 1.05. Sulfate and Smoke calculations use the refractive indices described in OPAC (Hess et al., 1998) and shown in Table 1.

Figure 3 provides Angstrom exponent spectra as a function of aerosol diameter to infer satellite derived aerosol size distribution characteristics and is a key improvement modeled in this approach (Malinina et al., 2019; Schuster et al., 2006). To expand on and help clarify the second solution space used to determine the coarse mode characteristics, new lines: 243–245, 247–248 are added.

Diverse stratospheric aerosol size distributions were tested as detailed in the original manuscript (new lines 253–254), with synthetic and observational data mapping well to the defined solution spaces. The results from this approach discussed in the original manuscript (see: sect. 6.2) highlight that the retrieved bimodal distributions are able to accurately describe a small and large particle mode comprising the majority of the number and mass concentrations of the aerosol distributions and minimizing the influence on extinction of the large particle mode. Retrieval results are valid for large coarse mode fractions, where increased magnitudes are shown to alter the aerosol optical and microphysical properties. Retrieval methods which use only a single mode are more heavily impacted by large particles due to their influence on aerosol mass, extinction, and volume, leading to suboptimal representation of aerosol size and number concentrations. Further validation is presented below.

#2. “The main issue with this paper is that the authors do not rigorously develop the retrieval method and show the advancement beyond other methods like, for example, Knepp et al., AMT, 2024 and the associated publicly released SAGE particle size product. The mathematical foundation for the retrieval with a clear case for robustness with respect to the retrieved parameters and discrimination of composition is required.”

The issues addressed in this manuscript are described in the work of Knepp et al., 2024 for the need to classify stratospheric aerosol size distributions of polydisperse populations and for stratospheric sulfate and smoke aerosols. Additionally, this work sought out to address occultation measurement size distribution retrievals having lower number densities when retrieving unimodal distributions as described in von Savigny & Hoffmann, 2020, impacting the retrieved microphysical properties. To the referee’s point on discrimination of aerosol composition, aerosol composition retrievals are outside of the scope of this manuscript. Thus, we highlight the retrieval results for assumptions of sulfate or smoke aerosol dominated layers. Aerosol layers filled with smoke make size distribution retrievals performed on assumptions of sulfate aerosols, as presented in Knepp et al., 2024 and done for the SAGE III/ISS operational product, doubtful particularly in the lower stratosphere.

We describe in the original manuscript a novel retrieval technique with the algorithm theoretical description and framework defined in sect. 3. Individual aerosol optical and microphysical properties (extinction, surface area density, volume density, effective diameter) and size distribution parameters (number density and coarse mode fraction) and the retrieved values are shown in the original manuscript in sects. 4–5. We present validation against stratospheric smoke samples and sulfate background in sect. 5 and 6. Sect. 6.1-6.2 discuss retrieval performance in detail. Validation of the retrieval methods are presented with strong agreement in the retrieved aerosol size distributions and microphysical properties against in situ measurements.

Revisions are made to clarify the methodology and retrieval approach and also highlight retrieval performance. Revisions described in response to comment #1 in new lines 226–229, 233–239, and 243–245, 247–248 expand and clarify descriptions on the solution spaces used to retrieve the bimodal lognormal distribution.

An analysis of the retrieval approach describe here with B^{2}SAP in situ measurements and the SAGE III/ISS version 6.0 operational product are presented below. New lines (590–593 and 672–674) are added to address the agreement between in situ and satellite retrieved aerosol microphysical properties using the approach here for stratospheric smoke. Fig. C3, presented below is added to the supplement to highlight the retrieval approach here against the in situ measurements and SAGE III/ISS operational aerosol product.

Figure C2–C5 show the retrievals described in this manuscript (SAGE III/ISS Sulfate or SAGE III/ISS Smoke), the operational SAGE III/ISS product (SAGE III/ISS v6), and in situ measurements from B^{2}SAP for 65 observations taken above Boulder, CO (40 °N, -105 °E) from 2019–2026 matching the coincidence criteria described in the original manuscript but increasing the temporal window to within 48 hours. In situ measurement sampling dates which do not have SAGE III/ISS observations meeting these spatiotemporal criteria are not included, while averages are calculated for SAGE III/ISS retrieved values over multiple coincident flights. Retrieved aerosol optical and microphysical properties are shown as mean values for each 0.5 km altitude bin over the period from 2019–2026 for observations meeting the coincidence criteria.

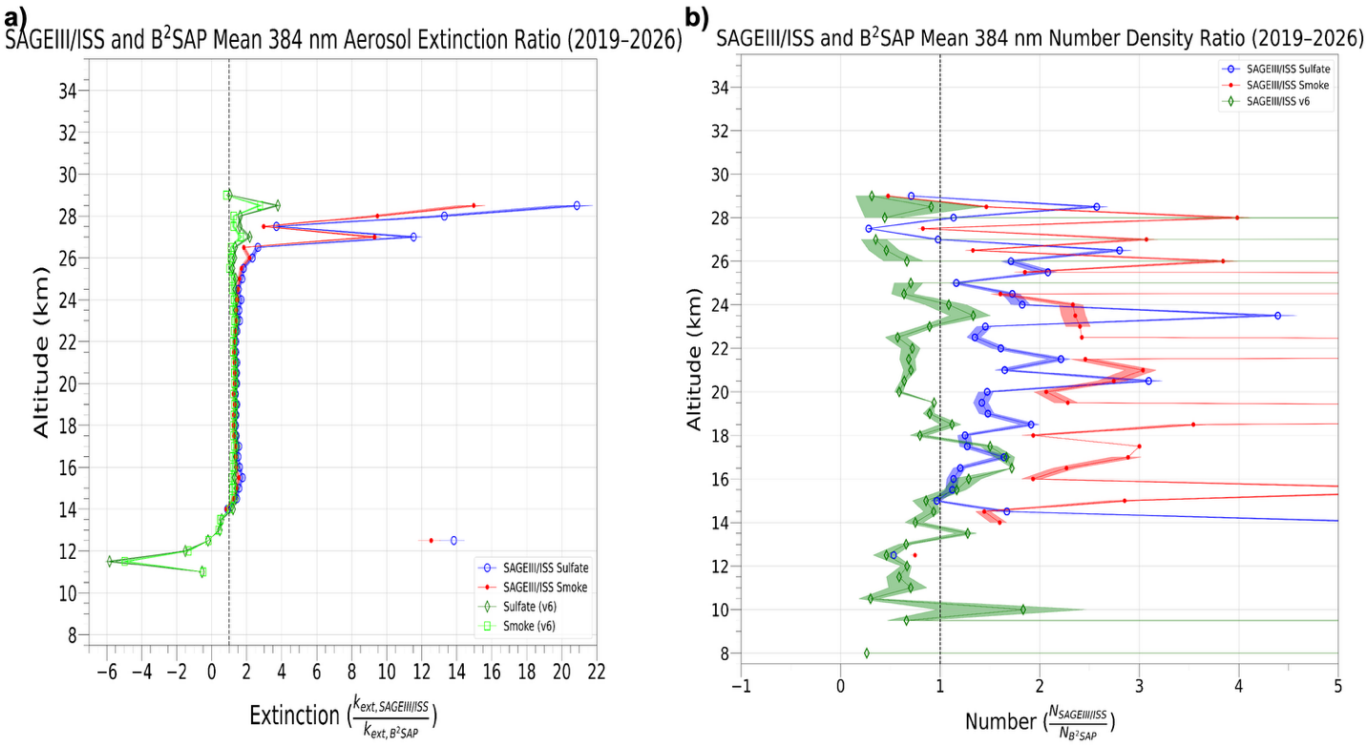

Figure C2: Ratios of SAGE III/ISS over B²SAP of a) 384 nm aerosol extinction coefficients and b) aerosol number density. SAGE III/ISS Sulfate and SAGE III/ISS Smoke refer to the approach described here, and SAGE III/ISS v6 refers to the operational product.

Figure C2 shows a) 384 nm extinction ratio and b) number density ratio for retrieved values from this work and the operational SAGE III/ISS v6 product compared to in situ values from B²SAP. Ratios vary from the 1:1 line in the retrieved microphysical properties in each retrieval approach largely due to differences in aerosol extinction shown in (a) between the satellite (this work and v6, respectively) and the in situ measurements. Aerosol extinction varies from the approach described here and the SAGE III/ISS v6 product only due to the strict uncertainty range of 20 % applied in use for the approach here, removing values which exceed this uncertainty range for any of the three diagnostic wavelength channels. Aerosol extinction is in fairly strong agreement between the satellite and in situ datasets, especially from 15–25 km, with increased values in the mean extinction profile for the approach used here. Aerosol extinction in the approach used here has larger increases above 23 km, and further above 26 km where it is increased over the v6 product and in situ values to a greater extent.

Aerosol number densities in (b) are more often underestimated by SAGE III/ISS v6 from the in situ measurement. Number densities are more often overestimated in the approach described here and for retrievals of smoke aerosols, respectively, when compared to the B²SAP retrieved size distributions assuming sulfate aerosols. Smoke aerosol number density and microphysical properties are shown here to account for intense wildfire seasons from 2019–2026 perturbing high altitude aerosol layers near Boulder, CO. Aerosol retrievals for smoke aerosol

concentrations are discussed in sect. 5 (new lines: 465–467, 496–497, 532–536) of the original manuscript comparing aerosol size distributions of smoke perturbed layers in the lower stratosphere from other stratospheric layers. For the in situ measurements presented here from B^2SAP, no condensation nuclei counter is flown to measure the total aerosol population ($N(d_p > 0.020\ \mu m)$). In situ aerosol number densities from B^2SAP are lower without measure of the small aerosol population, with the lower limit of aerosol size sensitivity being $N(d_p > 0.3\ \mu m)$, inflating the ratios of the number densities retrieved in the approach here presented in fig. C2b. Inclusion of CN measurements and channels measuring aerosol diameters of less than 300 nm can alter the number density as these channels describe the abundant small aerosol population, as shown in figure 13 in the original manuscript (new lines: 473-476).

Fig. C2 highlights the robustness of the solution presented in this work opposed to retrievals of unimodal aerosol size distributions from occultation instruments, i.e. number density retrievals are flawed due to underestimation of the total aerosol concentration due to extinction measurements being biased to the large particle concentrations. This work addresses the bias affecting the operational product in this regard and offers a new, more robust solution of the distribution mean aerosol extinction cross section, described in sect. 6.2 in new lines: 636–648. This leads to more confidence in the approach described here as the retrieved number densities are larger than the other instrument values while there still being strong agreement in the other aerosol properties, described below.

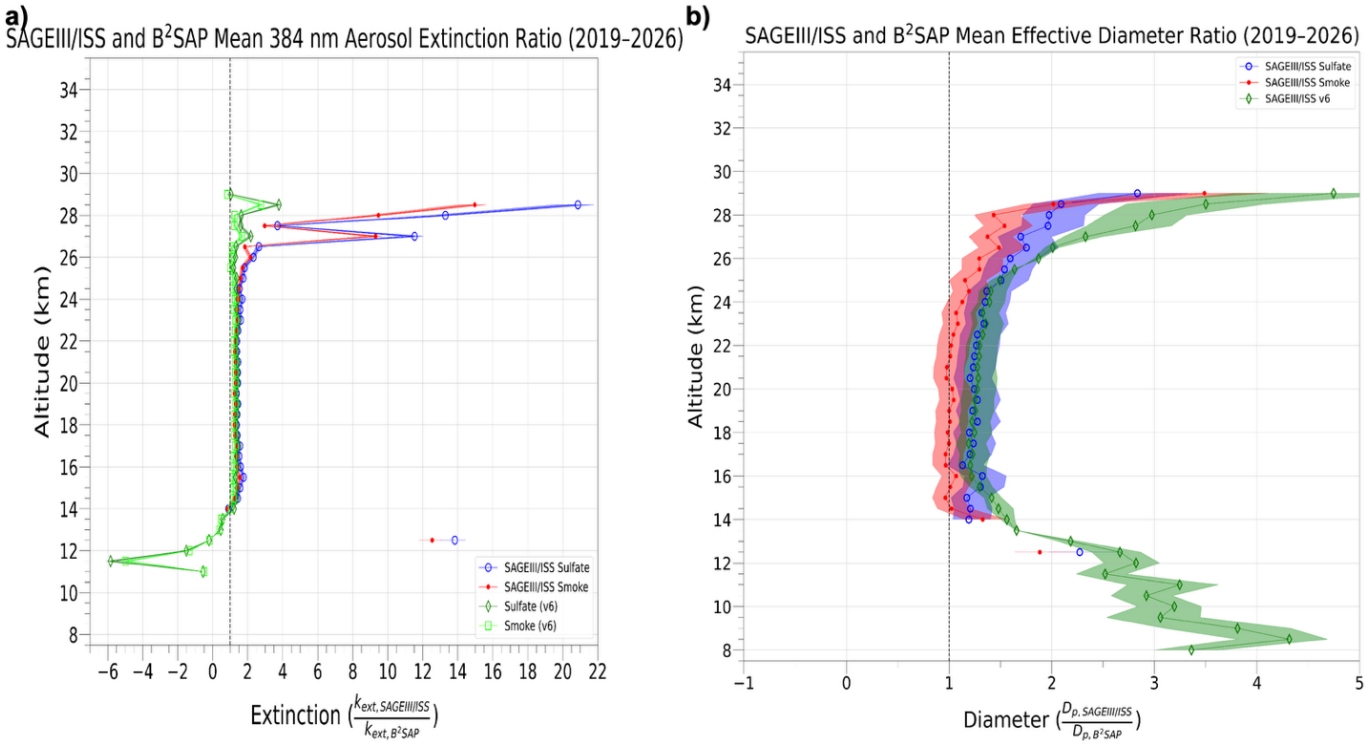

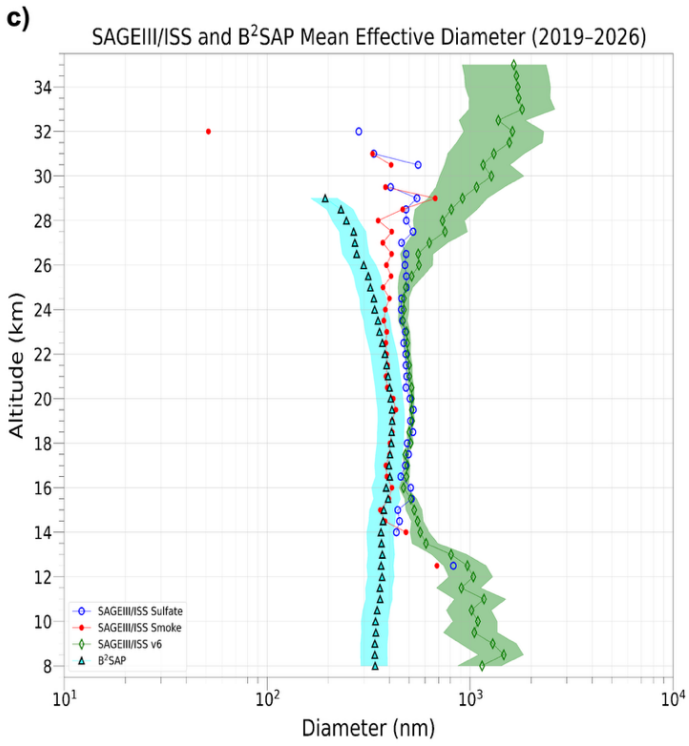

Figure C3: Ratios of SAGE III/ISS over B²SAP of a) 384 nm aerosol extinction coefficients and b) aerosol effective diameter. A vertical profile of mean aerosol effective diameters are presented in (c).

Figure C3 shows (a) 384 nm extinction ratio and (b) aerosol effective diameter ratio mean profiles over the same period. Higher altitudes (UTLS altitudes) display larger biases in the operational v6 product away from the in situ measurement and retrieval method described here as aerosol volumes decrease (increase). Aerosol effective diameters are clearly biased in the operational product due to the aforementioned large particle influence on extinction and inversion products. Retrievals using the approach here for sulfate and smoke aerosols are in better agreement with the in situ measurement. The better agreement with in situ measurements seen in the retrieved effective diameters using the approach here reinforces that the new retrieval approach can reliably determine the aerosol size distribution and higher level moments for polydisperse aerosol populations. Both a primary and secondary mode can be retrieved, lessening the reliance of the inversion to only a single mode of larger particles, and instead weighing the concentrations of the small and large particle modes in the retrieved distribution.

Figure C3 (c) presents the aerosol effective diameter mean profiles used in (b) to form the ratios. In situ and satellite retrieved aerosol effective diameters range from 200–600 nm in most layers. Sulfate retrievals agree well with the SAGE III/ISS v6 product from 15–25 km where the aerosol effective diameter is ~400–500 nm. Smoke aerosols display a smaller effective diameter ~300–400 nm which has strong agreement with the in situ profile. Sulfate and smoke aerosol size

sensitivity and retrieved diameters are described in sect. 3–5 of the original manuscript (new lines: 221–224, 355–359, 539–544), with smoke aerosols tending to be smaller than sulfate aerosols for moderately attenuated layers, but with pyroCb retrieved samples containing concentrations with larger diameters overall. The v6 product assuming sulfate aerosols overestimates aerosol diameter at higher and lower altitudes in comparison to the retrieval approach here and in situ measurement. Mean values for the approach described here are marginally increased at higher altitudes from the in situ measurement while remaining less than 600 nm, as the retrieved effective diameter increases as the measured extinction ratio increases.

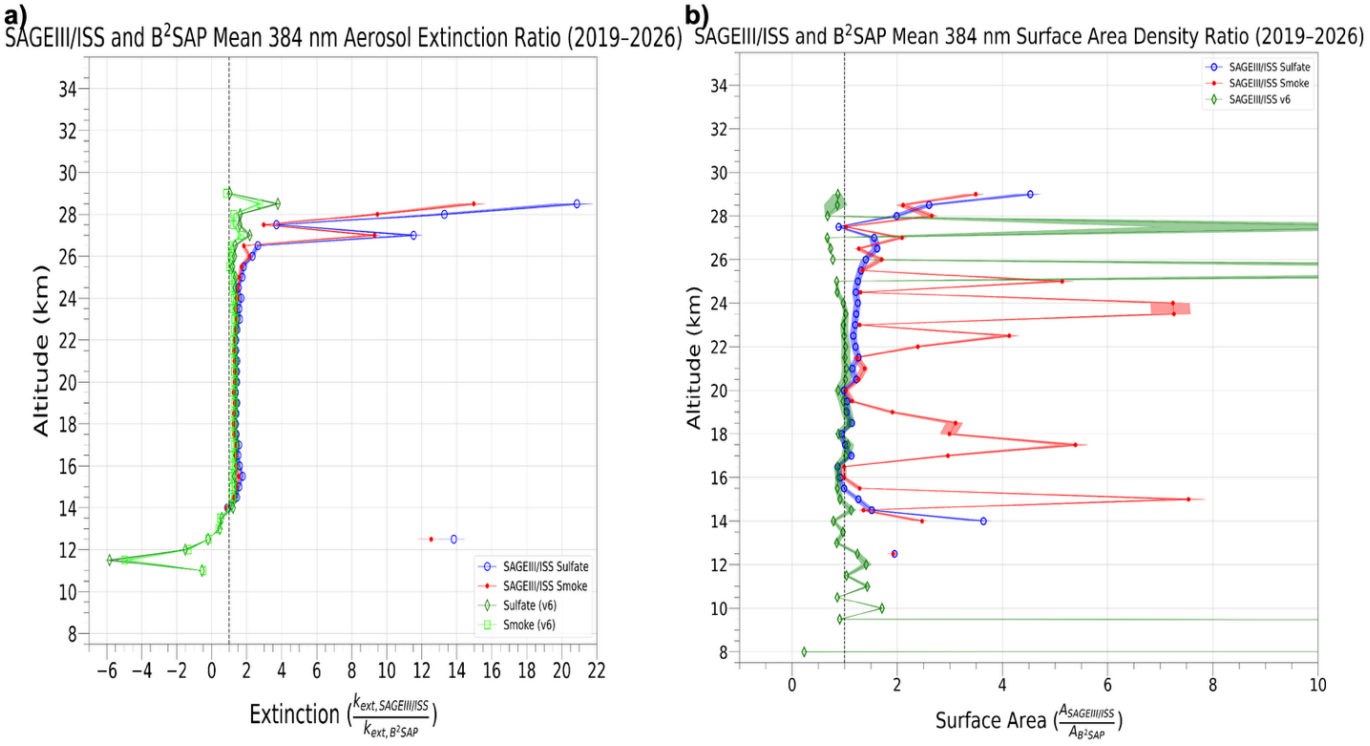

Figure C4: Ratios of SAGE III/ISS over B²SAP of a) 384 nm aerosol extinction coefficients and b) aerosol surface area density.

Figure C4 shows (a) 384 nm extinction ratio and (b) aerosol surface area density ratio mean profiles over the same period. Differences in the mean vertical profiles between the different approaches coincide with differences in the aerosol extinction profiles. Surface area density is highly sensitive to the retrieved aerosol size and number density. Retrievals from this approach for sulfate aerosols have increased surface area densities due to increased sensitivity to Aitken and fine mode aerosol concentrations. Overall, the approach here maintain larger surface area densities over the in situ measurement, matching the increases shown over the extinction ratio profile. Smoke aerosol mean surface area densities are more variable due in part to the lesser number of smoke samples throughout the sampling period, and smaller effective diameters of the retrieved size distributions from the sulfate retrievals in moderately attenuated layers.

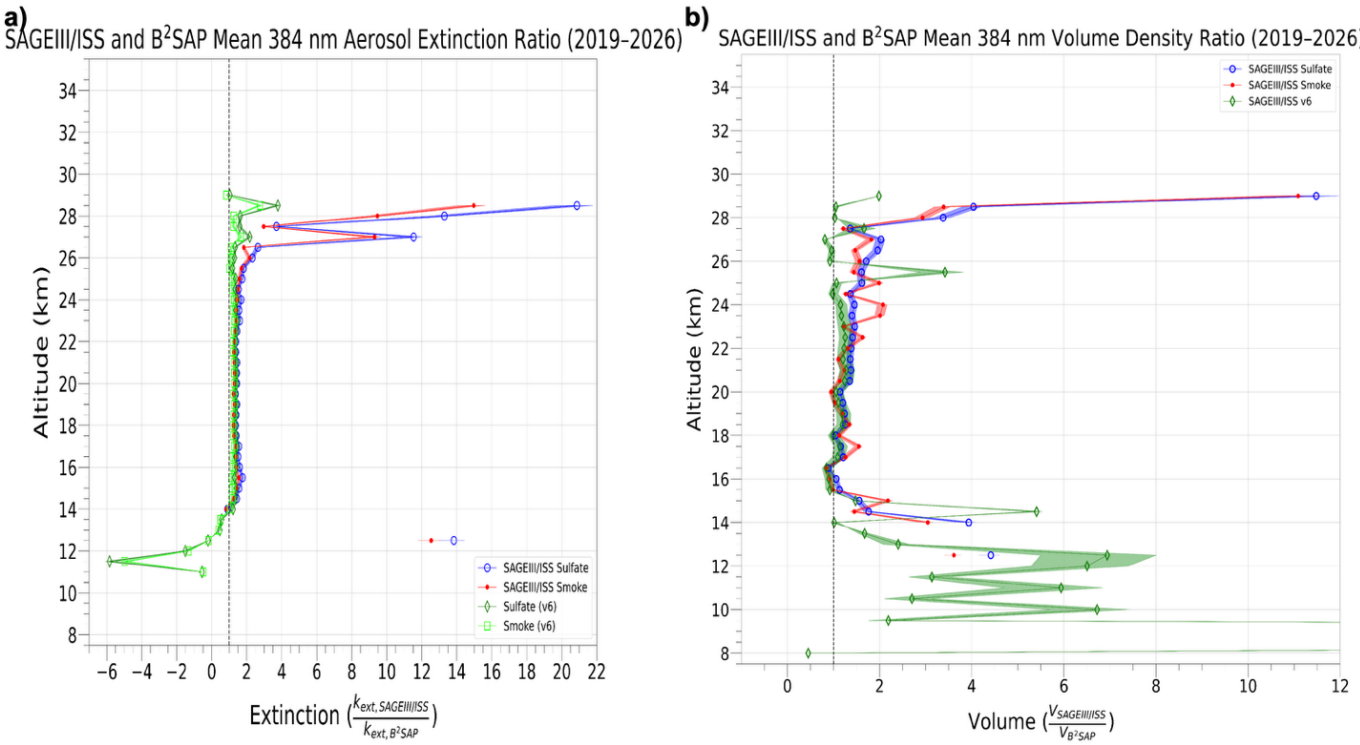

Figure C5: Ratios of SAGE III/ISS over B²SAP of a) 384 nm aerosol extinction coefficients and b) aerosol volume density.

Figure C5 shows (a) 384 nm extinction ratio and (b) aerosol volume density ratio mean vertical profiles over the same time period. Differences in the mean vertical profiles between the different approaches coincide with differences in the aerosol extinction profiles. The approach described here retains higher volume densities where there are increased extinction ratios. Volume densities generally show good agreement between the approaches. The approach here is able to resolve the lower stratospheric aerosol volume densities for both sulfate and smoke aerosols. Retrieved aerosol volume density at the top of the profile remains high as the extinction ratio is increased, but with retrieved aerosol effective diameters decreased from the v6 product and in closer agreement to the in situ measurement. The v6 product displays increased aerosol diameters and increased volume densities in comparison to the in situ product for high altitude, low concentration samples and low altitude mixed layers. The retrieval approach described here in contrast can minimize errors when there are lower aerosol concentrations. Low altitude mixed layers require more information to retrieve the aerosol size distribution due to higher uncertainties in the measured extinction coefficients.

Unimodal size distribution retrievals in instances of polydisperse aerosol populations are inherently biased to particles with high efficiency contributing to the overall extinction. Discrepancies in the microphysical properties during validation of a retrieval approach against in

situ measurement suggests potential inaccuracies in the retrieved distributions. Sufficiently broad aerosol distributions need aerosol concentrations to be partitioned into more than one mode to describe the lognormal distribution. Aerosol properties are determined to change for increases in large mode concentrations, displayed in figures 5–9 and discussed in sect. 4 and sects. 6.1, 6.2, and 7 in the original manuscript (new lines: 288–289, 579–580, 626–627, 714–716). Further, unimodal distributions do not correspond well with the long term historical record of stratospheric aerosols. Aerosol microphysical properties in the approach here show clear agreement with atmospheric values taken from in situ measurements, and overall agreement shown in fig. 18 are acknowledged in the revision with additional new lines: 672–674.

While the comparison of the approach documented here, and the SAGE III/ISS v6 operational product, and in situ measurements from B^2SAP from 2019–2026 are clearly viable, they do not fully represent the original scope of this work. Validation of the retrieval methods with in situ data for stratospheric smoke samples in the northern hemisphere midlatitudes are presented in section 5 of the original manuscript. The authors believe that retrievals of stratospheric aerosol size distributions must be capable of representing smoke aerosols due to frequent pyroCb events and severe wildfire activity. Furthermore, stratospheric aerosols are diverse in source and size and aerosol layer properties change when described by a unimodal versus bimodal distribution.

#3. “As part of this, the figures showing the results of the retrievals, Figures 5–10, need to be revised in a way that better shows the capability of the retrieval (with attention to figure creation, like for example in several cases the legend shows markers that correspond to a retrieval uncertainty and these are completely missing from the plot).”

We accept an update to figure 6a to the figure legend to match panels b–d. Figures 5–6 display the theoretical values and retrieval calculated values using the given number density of 10 cm^{-3}. This is done so that the retrieved value can be compared to the theoretical value and provide a fair assessment for each retrieval (with extinction bounded uncertainty range of ± 20 %).

The retrieved number densities following the simulated inversion are shown against the theoretical value of 10 cm^{-3} in figure 10. Figs. 7–10 are shown with uncertainty bars originating at the retrieved value and extending to the retrievals for measurements at the extinction uncertainty bounds of ± 20 %.

Fig. 6a has a revised legend to match panels b–d. Caption for fig. 7 on new line 316 is revised to match figs. 8-9. New lines 416–417 are added to the revised caption of fig. 10 to describe the retrieved number density for retrievals initiated at the bounds of the uncertainty range. New lines 645–646 are added to address the retrieval uncertainty presented in figure 5-6 with the extinction measurement and associated uncertainty range (± 20 %).

References

1. Knepp, T. N., Kovilakam, M., Thomason, L., and Miller, S. J.: Characterization of stratospheric particle size distribution uncertainties using SAGE II and SAGE III/ISS extinction spectra, Atmos. Meas. Tech., 17, 2025–2054, https://doi.org/10.5194/amt-17-2025-2024, 2024.
2. Malinina, E., Rozanov, A., Rieger, L., Bourassa, A., Bovensmann, H., Burrows, J. P., and Degenstein, D.: Stratospheric aerosol characteristics from space-borne observations: extinction coefficient and Ångström exponent, Atmos. Meas. Tech., 12, 3485–3502, https://doi.org/10.5194/amt-12-3485-2019, 2019.
3. Schuster, G. L., Dubovik, O., and Holben, B. N.: Angstrom exponent and bimodal aerosol size distributions, J. Geophys. Res. Atmos., 111, D07207, https://doi.org/10.1029/2005JD006328, 2006.
4. Wrana, F., von Savigny, C., Zalach, J., and Thomason, L. W.: Retrieval of stratospheric aerosol size distribution parameters using satellite solar occultation measurements at three wavelengths, Atmos. Meas. Tech., 14, 2345–2357, https://doi.org/10.5194/amt-14-2345-2021, 2021.
5. Wrana, F., Niemeier, U., Thomason, L. W., Wallis, S., and von Savigny, C.: Stratospheric aerosol size reduction after volcanic eruptions, Atmos. Chem. Phys., 23, 9725–9743, https://doi.org/10.5194/acp-23-9725-2023, 2023.
6. Wrana, F., Deshler, T., Löns, C., Thomason, L. W., and von Savigny, C.: Spatiotemporal variations of stratospheric aerosol size between 2002 and 2005 from measurements with SAGE III/M3M, Atmos. Chem. Phys., 25, 3717–3736, https://doi.org/10.5194/acp-25-3717-2025, 2025.